

Bose condensates in a harmonic trap near the critical temperature

T. Bergeman,¹ D. L. Feder,^{2,3} N. L. Balazs,¹ and B. I. Schneider⁴

¹*Physics Department, SUNY, Stony Brook, New York 11794-3800*

²*University of Oxford, Parks Road, Oxford OX1 3PU, United Kingdom*

³*National Institute of Standards and Technology, Gaithersburg, Maryland 20899-8410*

⁴*National Science Foundation, Arlington, Virginia 22230*

(Received 21 January 2000; published 11 May 2000)

The mean-field properties of finite-temperature Bose-Einstein gases confined in spherically symmetric harmonic traps are surveyed numerically. The solutions of the Gross-Pitaevskii (GP) and Hartree-Fock-Bogoliubov (HFB) equations for the condensate and low-lying quasiparticle excitations are calculated self-consistently using the discrete variable representation, while the most high-lying states are obtained with a local-density approximation. Consistency of the theory for temperatures through the Bose condensation point T_c requires that the thermodynamic chemical potential differ from the eigenvalue of the GP equation; the appropriate modifications lead to results that are continuous as a function of the particle interactions. The HFB equations are made gapless either by invoking the Popov approximation or by renormalizing the particle interactions. The latter approach effectively reduces the strength of the effective scattering length a_{sc} , increases the number of condensate atoms at each temperature, and raises the value of T_c relative to the Popov approximation. The renormalization effect increases approximately with the log of the atom number, and is most pronounced at temperatures near T_c . Comparisons with the results of quantum Monte Carlo calculations and various local-density approximations are presented, and experimental consequences are discussed.

PACS number(s): 03.75.Fi, 05.30.Jp, 05.10.-a

I. INTRODUCTION

Since the first observations of Bose-Einstein condensation (BEC) in dilute alkali-metal atom gases [1–3], experimental developments have posed many new tests for many-body theory, even though weakly interacting Bose gases have long been used as a textbook paradigm [4,5]. Numerous theoretical approaches have been employed in order to obtain accurate results for both the ground-state and nonequilibrium properties of the trapped Bose systems [6–8]. However, there have been notable differences between theoretical results and experimental data on the excitation frequencies near the transition temperature T_c [9–12]. This problem has inspired the introduction of a renormalized effective atom-atom interaction [11]. Recently developed theoretical approaches [13,14] that incorporate the dynamics of the non-condensate density but without a renormalized interaction have resulted in excitation frequencies in closer agreement with experiment. Nevertheless, the unresolved issues for Bose systems near T_c have provided a motivation for us to examine further the theoretical and numerical methods for modeling confined Bose gases near T_c . We have numerically implemented the most plausible and tractable equilibrium mean-field theories in order to systematically survey various properties of these systems.

In this work, we follow the standard mean-field theory [15], with certain modifications described in detail below. The nonlinear Gross-Pitaevskii (GP) equation, which includes interactions between the condensate and the thermal atoms, is solved for a static condensate containing N_c atoms. The eigenvalue of the GP equation, $\tilde{\mu}$, is usually identified with the thermodynamic chemical potential μ . The linear response of the system is represented by the Hartree-Fock-

Bogoliubov (HFB) equations, which yield the quasiparticle energies and amplitudes. These in turn determine the number of noncondensed atoms N_T as well as various coherence terms (thermodynamic averages over two or more Bose field operators). The GP and HFB equations are iterated to self-consistency at a given temperature T , subject to a fixed total number of atoms in the system $N = N_c + N_T$. As emphasized by Griffin [15], the coherence terms yield an excitation spectrum that is not gapless: the lowest-energy mode of the HFB equations has finite energy and does not coincide with the solution of the GP equation. The HFB-Popov (HFBP) approximation, which neglects these terms, has been quite successful in describing the properties of the trapped Bose gases, but is not well-grounded theoretically, and fails to yield accurate predictions for the low-lying excitations at high temperatures [9,12]. In this work, we explore a recently proposed extension of the HFBP theory that incorporates the coherence terms in a gapless manner [16,11]; in addition, we modify the commonly used identification of the chemical potential with the eigenvalue of the GP equation.

The identification of the chemical potential with the eigenvalue of the GP equation is incorrect in general. In the grand-canonical ensemble, the chemical potential is defined as $\mu = \partial E / \partial N$, corresponding to the energy cost E of adding a particle to the entire system, not only to the condensate. For a dilute, weakly interacting Bose gas at $T=0$, for which the population of noncondensed states (the depletion) is negligible, the identification $\tilde{\mu} = \mu$ is justified. At finite temperatures, however, the assumption yields results that are discontinuous as a function of the s -wave scattering length a_{sc} . To a better approximation, we find that the chemical potential at finite temperatures is given by the eigenvalue of the GP equation plus a term that varies inversely with the number of

condensate atoms. The resulting equations provide an improved description of these finite systems, yielding observables that are both continuous with a_{sc} and similar to those obtained using path-integral Monte Carlo techniques [17].

It is presently unclear to what extent many-body effects beyond the mean-field approximation modify the effective interactions among Bose-condensed atoms in harmonic traps [11,16,18,19]. For the homogeneous Bose gas, it is now established both from renormalization-group [20] and perturbation [21] theories that the many-body T matrix, or effective s -wave scattering length a , goes to zero at T_c . The low-energy, long-wavelength limit of the many-body T matrix has been shown to be closely related to the coherence term m_T [16,19]; this ‘‘anomalous average’’ represents two-particle correlations and is the Bose analog of the superconducting order parameter in interacting Fermi systems. Renormalizing the interaction using the m_T yields a gapless HFB theory without having to invoke the Popov approximation [11], but it remains uncertain whether the prescription is appropriate for nonuniform systems. The implications of this theory for trapped Bose condensates are explored numerically below, and the results are compared to those obtained with the Popov approximation and path-integral Monte Carlo methods.

In view of these somewhat conflicting results and unresolved issues, there is strong motivation for the continued development of numerical methods in order to implement various models and obtain quantitative predictions for comparison with experiment. Quantum Monte Carlo methods [17,22,23] are able to provide accurate results for certain observable quantities. The computational procedure is lengthy, however, and is not demonstrably able to yield excitation frequencies since it typically applies only to equilibrium configurations. Local-density approximations (LDA) are much simpler to apply, but the standard forms fail near T_c and are questionable when the density is so small that the local collision rate is insufficient to establish local thermodynamic equilibrium. On the other hand, widely used basis-set techniques are generally unable to represent the large numbers of atoms in excited states at high temperatures. Recently, Reidl *et al.* [24] have used (for 2000 Rb atoms at $T = 0.5T_c$) a hybrid method in which a sum over discrete quasiparticle states at low energies is supplemented by an integral over an energy-dependent LDA above some cutoff energy. The interactions of these two subensembles with each other are expressed by mean-field potentials that represent the effect of background atoms. In the present work, the low-lying states are obtained by solving the HFB equations using the discrete variable representation (DVR) [25–27] and the cutoff energy is raised until the results converge to within a stated tolerance. The techniques employed have enabled the investigation of trapped Bose gases at finite temperatures containing a larger number of atoms than in previous calculations that we are aware of. As a result, the approach of these systems to the local thermodynamic equilibrium and to the hydrodynamic limit can be explored.

In Sec. II A, we outline the GP and HFB equations. We discuss the chemical potential and gapless theories in Secs. II B and II C, respectively. Section II D reviews LDA meth-

ods both as alternative approaches for comparison purposes and the complementary use for the most energetic atoms. In Sec. III, we discuss our numerical methods and iteration procedures. Section IV presents results for Bose atoms in a spherically symmetric harmonic trap as a function of the scaled s -wave scattering length, total number of atoms, and temperature.

II. THEORETICAL FRAMEWORK

A. Thermal sums over quasiparticle states

The derivation of mean-field equations for a weakly interacting, dilute Bose gas has been described in detail elsewhere [28–30,15]. The question of the chemical potential for $T > 0$ for thermal sums of quasiparticle states deserves more thorough discussion, however, and we modify the standard procedure. In addition, following discussions by Burnett *et al.* [16,11,19], we treat the anomalous (coherence) terms m_T in a manner that produces a ‘‘gapless’’ theory.

Following the standard approach, we decompose the Bose field operator into a c number for the condensate, plus an operator representing its fluctuations. The full many-body Hamiltonian is approximated using mean-field theory, becoming explicitly number-nonconserving. The grand-canonical ensemble is used, and thus the chemical potential, μ , and temperature, T , are the sole fixed quantities. The generalized Gross-Pitaevskii (GP) equation for the condensate and coupled Bogoliubov equations for the excited quasiparticle states are then solved. For a finite number of atoms in a harmonic potential, however, the standard approach yields values for the mean condensate number N_c that are discontinuous as a function of interaction strength a_{sc} . In our approach, the eigenvalue of the GP equation, $\tilde{\mu}$, is determined by the mean number of atoms in the condensate N_c . In contrast, the chemical potential, μ , is adjusted so that the mean *total* number of atoms is the desired value. A simple relationship is found connecting $\tilde{\mu}$, μ , and N_c , which is adapted from the ideal Bose gas case.

The Hamiltonian for an interacting Bose gas in a trap in the grand-canonical ensemble is

$$\hat{H} - \mu \hat{N} = \int d\mathbf{r} \left\{ \hat{\psi}^\dagger \left[-\frac{\hbar^2}{2M} \nabla^2 + V_{\text{ext}} - \mu \right] \hat{\psi} + \frac{g}{2} \hat{\psi}^\dagger \hat{\psi}^\dagger \hat{\psi} \hat{\psi} \right\}, \quad (1)$$

where the field operator $\hat{\psi}(\mathbf{r})$ satisfies $[\hat{\psi}(\mathbf{r}_1), \hat{\psi}^\dagger(\mathbf{r}_2)] = \delta(\mathbf{r}_1 - \mathbf{r}_2)$. The pseudopotential atom-atom interaction has been chosen to be $V(\mathbf{r}_1 - \mathbf{r}_2) = g \delta(\mathbf{r}_1 - \mathbf{r}_2)$, where the coupling constant $g = 4\pi \hbar^2 a_{sc} / M$ is written in terms of the scattering length a_{sc} and mass M . The harmonic potential is $V_{\text{ext}} = \frac{1}{2} M \omega_0^2 r^2$ with trapping frequency ω_0 assumed to be isotropic.

The Hamiltonian may be rewritten as

$$\begin{aligned} \hat{H} - \mu \hat{N} &= H - \tilde{\mu} \hat{N} + (\tilde{\mu} - \mu) \hat{N} \\ &= \hat{K} + (\tilde{\mu} - \mu) \hat{N}, \end{aligned} \quad (2)$$

where, as mentioned above, the Lagrange multiplier $\tilde{\mu}$ is related to the number of atoms in the condensate. In the following, we choose to diagonalize the operator $\hat{K} = \hat{H} - \tilde{\mu}\hat{N}$ rather than the original $\hat{H} - \mu\hat{N}$; both choices must lead to the same excitation spectrum, though with a temperature-dependent shift of the vacuum for quasiparticle excitations. In order to make further progress, the Bose field operator $\hat{\psi} = \Phi + \hat{\phi}$ is now decomposed into Φ , a c number for the condensate, and $\hat{\phi}(\mathbf{r})$, which annihilates a thermal atom at \mathbf{r} . The condensate density is defined by $n_c = |\Phi|^2$, and the number of condensate atoms is $N_c = \int d\mathbf{r} |\Phi(\mathbf{r})|^2$. The noncondensate (thermal) density n_T and anomalous (coherence) terms m_T and \tilde{m}_T are [15]

$$n_T = \langle \hat{\phi}^\dagger \hat{\phi} \rangle, \quad m_T = \langle \hat{\phi} \hat{\phi} \rangle, \quad \tilde{m}_T = \langle \hat{\phi}^\dagger \hat{\phi}^\dagger \rangle, \quad (3)$$

where the angular brackets indicate a thermal average in the grand-canonical ensemble, discussed in more detail below. The mean-field approximation is used to reduce the third- and fourth-order terms to, respectively, first and second order in $\hat{\phi}, \hat{\phi}^\dagger$ so that the Hamiltonian \hat{K} can be diagonalized, following the procedure normally used for $\hat{H} - \mu\hat{N}$ [28,15].

Excluding the possibility of aggregate motion and vortices [29], Φ may be taken to be real. The first-order terms (plus third-order terms in the mean-field approximation) in \hat{K} vanish if the equation for the condensate is taken to be the generalized GP equation:

$$\left[-\frac{\hbar^2}{2M} \nabla^2 + V_{\text{ext}} + g[n_c + 2n_T + \tilde{m}_T] \right] \Phi = \tilde{\mu} \Phi. \quad (4)$$

Note that $\tilde{\mu}$ is the eigenvalue of the GP equation. The part of \hat{K} that is zeroth order in the excited orbitals is a c number

$$K_0 = \int d\mathbf{r} \Phi(\mathbf{r}) \left(-\frac{\hbar^2}{2M} \nabla^2 + V_{\text{ext}} - \tilde{\mu} + \frac{g}{2} |\Phi(\mathbf{r})|^2 \right) \Phi(\mathbf{r}). \quad (5)$$

The terms in \hat{K} that are second order in $\hat{\phi}$ are (in the mean-field approximation) diagonalized by the canonical transformation

$$\begin{aligned} \hat{\phi}(\mathbf{r}) &= \sum_j [u_j(\mathbf{r}) \hat{\alpha}_j + v_j^*(\mathbf{r}) \hat{\alpha}_j^\dagger], \\ \hat{\phi}^\dagger(\mathbf{r}) &= \sum_j [u_j^*(\mathbf{r}) \hat{\alpha}_j^\dagger + v_j(\mathbf{r}) \hat{\alpha}_j], \end{aligned} \quad (6)$$

such that $[\hat{\alpha}_i, \hat{\alpha}_j^\dagger] = \delta_{i,j}$. The operator \hat{K} is diagonal to second order in $\hat{\phi}$ if the quasiparticle amplitudes $u_j(\mathbf{r})$ and $v_j(\mathbf{r})$ are solutions of the Bogoliubov coupled equations

$$\begin{aligned} \hat{L}u_j(\mathbf{r}) + \mathcal{Q}(\mathbf{r})v_j(\mathbf{r}) &= \epsilon_j u_j(\mathbf{r}), \\ \hat{L}v_j(\mathbf{r}) + \mathcal{Q}(\mathbf{r})u_j(\mathbf{r}) &= -\epsilon_j v_j(\mathbf{r}), \end{aligned} \quad (7)$$

where $\hat{L} = K + V_{\text{ext}} - \tilde{\mu} + 2gn(\mathbf{r})$, $\mathcal{Q} = g[n_c(\mathbf{r}) + m_T(\mathbf{r})]$, and the total density is $n(\mathbf{r}) = n_c(\mathbf{r}) + n_T(\mathbf{r})$. For gapless theories, discussed further below, the $j=0$ ‘‘Goldstone mode’’ has the property $\epsilon_0 = 0$, so that $u_0(\mathbf{r}) = -v_0(\mathbf{r}) = \Phi(\mathbf{r})$. Thus on the ϵ_j energy scale, the condensate has zero energy and defines the vacuum for quasiparticle excitations.

After the substitution, $\hat{\psi} = \Phi + \hat{\phi}$, the number operator $\hat{N} = \int d\mathbf{r} \hat{\psi}^\dagger(\mathbf{r}) \hat{\psi}(\mathbf{r})$ contains terms, such as $\int d\mathbf{r} \Phi \hat{\phi}$, that do not conserve particle number. The Bogoliubov transformation (6) and coupled equations (7) introduce a quasiparticle basis such that terms $\hat{\alpha}_j^\dagger \hat{\alpha}_j^\dagger$ and $\hat{\alpha}_j \hat{\alpha}_j$ are eliminated, so the *quasi-particle* number is conserved [28]. The diagonalized Hamiltonian explicitly does not conserve particle number, however; the operator \hat{K} in the quasiparticle basis does not commute with the excited particle number operator $\hat{\phi}^\dagger \hat{\phi}$, which has contributions from $\hat{\alpha}_j^\dagger \hat{\alpha}_j^\dagger$ and $\hat{\alpha}_j \hat{\alpha}_j$ terms. In the grand-canonical ensemble, only T and μ are precisely defined, and all observables must be defined in terms of thermal averages. Each occupation number, including the condensate number, fluctuates about its mean value

$$\langle \hat{N}_j \rangle \equiv \langle \hat{\alpha}_j^\dagger \hat{\alpha}_j \rangle, \quad j=0,1,\dots, \quad (8)$$

where the explicit definition of the average $\langle \hat{O} \rangle$ is yet undefined. Similarly, both the eigenvalue $\tilde{\mu}$ of the GP equation (4) and the total energy $\langle E \rangle$ fluctuate about their mean values.

Inserting the transformation (6) into Eqs. (3) and introducing the identification given by Eq. (8), the normal and anomalous densities become

$$n_T(\mathbf{r}) = \sum_{j=1} \{ \langle \hat{N}_j \rangle [|u_j(\mathbf{r})|^2 + |v_j(\mathbf{r})|^2] + |v_j(\mathbf{r})|^2 \}, \quad (9)$$

$$m_T(\mathbf{r}) = \sum_{j=1} u_j(\mathbf{r}) v_j^*(\mathbf{r}) [2 \langle \hat{N}_j \rangle + 1]. \quad (10)$$

The standard normalization $\int d\mathbf{r} [|u_j(\mathbf{r})|^2 - |v_j(\mathbf{r})|^2] = 1$ yields

$$\int d\mathbf{r} [|u_j(\mathbf{r})|^2 + |v_j(\mathbf{r})|^2] \equiv 1 + 2V_j, \quad (11)$$

where $V_j = \int d\mathbf{r} |v_j(\mathbf{r})|^2$. The quantities V_j are related to the $T=0$ depletion, which is $\sum_{j=1} V_j$. The relation between the total atom number and the quasiparticle occupation numbers is therefore

$$\begin{aligned} \langle \hat{N} \rangle &\equiv N_c + N_T = \langle N_0 \rangle + \int d\mathbf{r} n_T(\mathbf{r}) \\ &= N_c + \sum_{j=1} [\langle \hat{N}_j \rangle (1 + 2V_j) + V_j], \end{aligned} \quad (12)$$

where the average number of atoms is written in terms of a contribution from the condensate and noncondensate (excitations).

The thermal average of the diagonalized Hamiltonian then becomes

$$\begin{aligned} \langle \hat{H} - \mu \hat{N} \rangle &= K_0 + \sum_{j=1} \epsilon_j (\langle \hat{N}_j \rangle - V_j) + (\tilde{\mu} - \mu) \langle \hat{N} \rangle \\ &= E_c - \mu N_c + \sum_{j=1} \{ \langle \hat{N}_j \rangle [\epsilon_j + (\tilde{\mu} - \mu)(1 + 2V_j)] \\ &\quad + V_j (\tilde{\mu} - \mu - \epsilon_j) \}, \end{aligned} \quad (13)$$

where $E_c = K_0 + \tilde{\mu} N_c$ is the total ground state, or condensate, energy.

B. Occupation factors and the chemical potential

In the Bogoliubov approach, the ensemble is considered to be the sum of a condensate plus noninteracting quasiparticles. The mean occupation numbers of the quasiparticle states are to be determined from the grand partition function,

$$\Omega = \text{Tr} \{ \exp[-\beta (\hat{H} - \mu \hat{N})] \}, \quad (14)$$

through the standard identities [4,5]

$$\langle N \rangle = \frac{1}{\beta} \left(\frac{\partial \ln \Omega}{\partial \mu} \right)_T, \quad \langle E \rangle = - \left(\frac{\partial \ln \Omega}{\partial \beta} \right)_{\mu, T}. \quad (15)$$

Unfortunately, while the diagonalized Hamiltonian is written in terms of noninteracting single-quasiparticle energies, the expressions (12) and (13) involve the thermal averages of particle occupation that we are now seeking to determine. Furthermore, the factorization that one makes for an ideal Bose gas is invalid for a gas of interacting Bose atoms because the quasiparticle energies depend on the occupation numbers, as well as the reverse. Thus, rigorously, these occupation factors should be calculated self-consistently, along with Eqs. (4) and (7), since they depend on as well as *determine* the quasiparticle eigenvalues [31]. To do so analytically would be a truly daunting task. We make several simplifying assumptions in order to obtain results, but we emphasize that these questions merit further study.

In reality, the probabilities $\langle \hat{N} \rangle$ will be peaked at the most probable values, as discussed below for the condensate. Therefore, when evaluating the sum over N_j in Eq. (14), deviations of $N_{j'}$ from $\langle \hat{N}_{j'} \rangle$ for $j' \neq j$ will not greatly modify the spectrum of the quasiparticle states. If this is so, a reasonable approximation is to replace $\langle \hat{N}_j \rangle$ by N_j when estimating the mean occupation numbers from the grand partition function. If the dependence of ϵ_j and N_j on $N_{j'}$ ($j \neq j'$) is also neglected, then Ω can be factored, and we obtain

$$\begin{aligned} \langle N_j \rangle &= \frac{\sum_{N_j} N_j \exp\{ -\beta [\epsilon_j + (\tilde{\mu} - \mu)(1 + 2V_j)] N_j \}}{\sum_{N_j} \exp\{ -\beta [\epsilon_j + (\tilde{\mu} - \mu)(1 + 2V_j)] N_j \}} \\ &\approx \frac{1}{\exp\{ \beta [\epsilon_j + (\tilde{\mu} - \mu)(1 + 2V_j)] \} - 1}, \quad \forall j. \end{aligned} \quad (16)$$

In order to obtain the result on the second line of Eq. (16), the population dependences of the GP eigenvalue $\tilde{\mu}$ and the quasiparticle energies ϵ_j are ignored. At sufficiently low temperatures, the ϵ_j for trapped Bose condensates are relatively insensitive to the value of N_c and the temperature; indeed, in the Thomas-Fermi (TF) limit, valid for large condensates, the excitation frequencies at zero temperature are independent of N_c .

Neglecting the factors V_j , and shifting the energy scale so that $E_j \equiv \epsilon_j + \tilde{\mu}$, one recovers the more conventional expression

$$\langle N_j \rangle = \frac{1}{\exp[\beta(E_j - \mu)] - 1}. \quad (17)$$

From this expression (17) for $j=0$, with $E_0 = \tilde{\mu}$, one finds that the chemical potential μ and the eigenvalue of the GP equation $\tilde{\mu}$ are related by the expression

$$\mu = \tilde{\mu} - \frac{1}{\beta} \ln \left(1 + \frac{1}{N_c} \right), \quad N_c > 0. \quad (18)$$

For $T=0$ this gives the usual definition $\tilde{\mu} = \mu$, but for $T > 0$ there is a correction to μ that increases as N_c decreases. While this additional term will not be correct at high temperatures where the condensate is strongly depleted, it will be shown below that results obtained with this procedure are continuous functions of a_{sc} at all temperatures, while with $\mu = \tilde{\mu}$ they are not.

It is difficult to go beyond the above approximations, but we will suggest possible avenues to proceed in future work. The major effect omitted is the dependence of the quasiparticle energies, E_j (including $E_0 = \tilde{\mu}$) on N_c . One can first consider the condensate term itself. We assume, for the moment, that factorization of Ω (14) is valid, and write

$$\Omega = \Omega_c \Omega_T, \quad \Omega_c = \sum_{N_c} e^{\beta(\mu N_c - E_c)}. \quad (19)$$

In the Thomas-Fermi approximation (kinetic energy in the GP equation neglected), one obtains for a spherical condensate [6]

$$\tilde{\mu}_{\text{TF}} = \frac{1}{2} \left(\frac{15 N_c a_{sc}}{a_0} \right)^{2/5} \equiv \gamma N_c^{2/5}, \quad (20)$$

where the harmonic-oscillator length is $a_0 = \sqrt{\hbar/M\omega}$. The following relations follow in the same approximation:

$$E_c = \frac{5}{7} \gamma N_c^{7/5} = \frac{5}{7} \tilde{\mu}_{\text{TF}} N_c, \quad \frac{\partial E_c}{\partial N_c} = \tilde{\mu}. \quad (21)$$

Then from Eq. (19), neglecting Ω_T , one can obtain the mean value of the condensate occupation from $\langle N_c \rangle = \sum_N N_c P(N_c) / \sum_N P(N_c)$, where $P(N_c) = \exp[\beta(\mu N_c - \frac{5}{7} \gamma N_c^{7/5})]$. We have verified numerically for typical values of β and μ that the mean value is extremely close to the most probable value \bar{N}_c for which $P(N_c)$ is maximum. Furthermore, an expansion of the exponent in the above expression for $P(N_c)$ yields a value for the variance of N_c , interpreted as the value of σ such that $P(\bar{N}_c \pm \sigma) = (1/e)P(\bar{N}_c)$. In the grand-canonical ensemble at zero temperature, therefore, one obtains $\langle \delta N_c \rangle = \sqrt{(5/7\beta\gamma)} \bar{N}_c^{3/10}$, so that the fractional width of the occupation number distribution decreases as $\bar{N}_c^{-7/10}$. This may be compared with the result of Giorgini *et al.*, derived from excited-state occupation numbers for the canonical ensemble, $\langle \delta N_c \rangle \sim (T/T_c) N_c^{2/3}$ [32]. Either result confirms that the fluctuations in N_c are relatively small for large N_c . One should next consider how the dependence of Ω_T would effect $\langle N_c \rangle$ and $\langle \delta N_c \rangle$. This is left for future work.

The dependence of the quasiparticle states on the occupation factors reflects the extensive nature of this finite interacting system; that is, adding a particle to the many-body system alters both the number and character of the accessible states. This behavior is similar [33,34] to that of a finite gas of noninteracting particles obeying *fractional exclusion statistics* [35], which obey a statistics intermediate between that of bosons and fermions. The parameter representing the statistics has been identified with the strength of the δ -function potential for an interacting trapped Bose gas in two dimensions [34]. Indeed, our expression (18) for the thermodynamic chemical potential is similar to that found for a noninteracting fractional-statistics gas at finite temperature [33,34]. We hope to pursue these issues more fully in future work.

C. Gapless approximations

We return to the conditions for gaplessness. The GP (4) and Bogoliubov (7) equations together comprise the ‘‘Hartree-Fock-Bogoliubov’’ (HFB) approximation for a dilute interacting Bose gas. In this case, one does not obtain $\epsilon_0 = 0$, and the theory is said to not be gapless (the term has been taken from the homogeneous situation). In the Popov approximation, gaplessness is ensured by neglecting the coherence terms m_T and \tilde{m}_T , but the justification for such an approximation is questionable [15].

In order to convert HFB into a gapless theory and still retain the anomalous averages, Burnett *et al.* [16,11] have recently proposed an alternative treatment in which the coupling functions for the condensate $g_c(\mathbf{r})$ and excited states $g_e(\mathbf{r})$ absorb the pairing correlations, and thereby take on a spatial dependence. Equation (4) becomes

$$\{K + V_{\text{ext}} + g_c n_c + 2g_e n_T\} \Phi = \tilde{\mu} \Phi, \quad (22)$$

and similarly, $\hat{\mathcal{L}}$ and \mathcal{Q} appearing in Eqs. (7) become

$$\hat{\mathcal{L}} = K + V_{\text{ext}} - \tilde{\mu} + 2g_c n_c + 2g_e n_T, \quad \mathcal{Q} = g_c n_c. \quad (23)$$

In the proposed gapless theories, labeled *G1*, and *G2*, the coupling constants are chosen to be

$$\{g_c; g_e\} = \begin{cases} \{g_1; g\}, & G1 \\ \{g_1; g_1\}, & G2, \end{cases} \quad (24)$$

where

$$g_1(\mathbf{r}) = g \left[1 + \frac{m_T(\mathbf{r})}{n_c(\mathbf{r})} \right]. \quad (25)$$

The renormalized coupling g_1 replaces the two-body T matrix associated with binary atomic collisions, which is the scattering length a_{sc} *in vacuo*, by the zero momentum and energy limit of the homogeneous many-body T matrix [16,11,19]. In the *G1* approximation, only the condensate-condensate and condensate-excited are dressed, while *G2* is motivated by the expectation that all particle interactions should be similar. Renormalization of the coupling has the additional advantage of removing the ultraviolet divergence in m_T resulting from high-energy quasiparticle contributions of Eq. (10) in the T -matrix approximation. In nonuniform systems such as the trapped Bose gases, however, the value of $g_1(\mathbf{r})$ can diverge in regions near the condensate surface where the condensate density vanishes more rapidly than the anomalous average. In practice, this divergence may be eliminated by setting $g_1(\mathbf{r}) = g \{1 + m_T(\mathbf{r})/[n_c(\mathbf{r}) + \delta]\}$, where $\delta \approx 10^{-2}$. While the results, described in detail below, are found not to depend strongly on the choice of δ , its existence underlines a deficiency in the theory in its present form. The consequences of the *G1* approximation are not explored in this work. In the following, the notation $g(\mathbf{r})$ will be used in place of $g_1(\mathbf{r})$ and in distinction from g , which is unrenormalized.

D. Local-density approximation

In local-density-approximation (LDA) schemes, the condensate density is assumed to be varying sufficiently slowly that the population of excited states is determined entirely by the local potential and temperature. The thermal density may then be treated locally as if the interacting Bose gas were homogeneous. We will discuss three basic LDA schemes and several variants.

In the semiclassical approximation to the GP and HFB equations [24,36], the thermal atom quasiparticle amplitudes in the Bogoliubov equations (7) become local functions $u(\mathbf{p}, \mathbf{r})$ and $v(\mathbf{p}, \mathbf{r})$. With the Popov approximation, one obtains the coupled algebraic equations

$$\begin{pmatrix} \mathcal{L}(\mathbf{p}, \mathbf{r}) & g n_c(\mathbf{r}) \\ -g n_c(\mathbf{r}) & -\mathcal{L}(\mathbf{p}, \mathbf{r}) \end{pmatrix} \begin{pmatrix} u(\mathbf{p}, \mathbf{r}) \\ v(\mathbf{p}, \mathbf{r}) \end{pmatrix} = \epsilon(\mathbf{p}, \mathbf{r}) \begin{pmatrix} u(\mathbf{p}, \mathbf{r}) \\ v(\mathbf{p}, \mathbf{r}) \end{pmatrix}, \quad (26)$$

where $\mathcal{L}(\mathbf{p}, \mathbf{r}) = p^2/2m + V_{\text{ext}}(\mathbf{r}) - \tilde{\mu} + 2gn(\mathbf{r})$. With the condition $u(\mathbf{p}, \mathbf{r})^2 - v(\mathbf{p}, \mathbf{r})^2 = 1$, the local excitation energies may be immediately obtained, $\epsilon(\mathbf{p}, \mathbf{r}) = [\mathcal{L}(\mathbf{p}, \mathbf{r})^2 - g^2 n_c^2(\mathbf{r})^2]^{1/2}$, and have the well known linear dispersion. The noncondensate density from Eq. (9) may then be easily found [24]:

$$n_T(\mathbf{r}) = \int \frac{d^3 \mathbf{p}}{(2\pi)^3} \left[\frac{\mathcal{L}(\mathbf{p}, \mathbf{r})}{\epsilon(\mathbf{p}, \mathbf{r})} \left(\langle n(\mathbf{p}, \mathbf{r}) \rangle + \frac{1}{2} \right) - \frac{1}{2} \right] \times \Theta(\mathcal{L}(\mathbf{p}, \mathbf{r})^2 - g^2 n_c^2(\mathbf{r})), \quad (27)$$

where

$$\langle n(\mathbf{p}, \mathbf{r}) \rangle = \frac{1}{\exp[\beta(\epsilon(\mathbf{p}, \mathbf{r}) + \tilde{\mu} - \mu)] - 1}, \quad (28)$$

such that the Θ function is unity when the argument is positive, and zero otherwise. These equations define the Hartree-Fock Bogoliubov Popov LDA, which we will refer to as the ‘‘BPLDA.’’ For $G2$ calculations, one obtains the BGLDA by the substitution $g \rightarrow g(\mathbf{r})$ everywhere. Then one needs

$$m_T(\mathbf{r}) = \int \frac{d^2 \mathbf{p}}{(2\pi)^3} u(\mathbf{p}, \mathbf{r}) v(\mathbf{p}, \mathbf{r}) [2\langle n(\mathbf{p}, \mathbf{r}) \rangle + 1] \\ = -g(\mathbf{r}) n_c(\mathbf{r}) \int \frac{d^3 \mathbf{p}}{(2\pi)^3} \frac{1}{2\epsilon} [2\langle n(\mathbf{p}, \mathbf{r}) \rangle + 1] \\ \times \Theta(\mathcal{L}(\mathbf{p}, \mathbf{r})^2 - g^2 n_c^2(\mathbf{r})). \quad (29)$$

The integral is not formally convergent, however. Since the anomalous averages appear only in the context of the $G1$ and $G2$ approximations, where the formal ultraviolet divergence is eliminated, we may safely neglect the $+1$ term following the $2\langle n(\mathbf{p}, \mathbf{r}) \rangle$.

The semiclassical HFBP approximation exhibits a gapless excitation spectrum only if the condensate is also treated within the LDA, which implies the TF density:

$$n_c(\mathbf{r}) = \frac{\tilde{\mu} - V_{\text{ext}}(\mathbf{r}) - 2gn_T(\mathbf{r})}{g} \Theta[\tilde{\mu} - V_{\text{ext}}(\mathbf{r}) - 2gn_T(\mathbf{r})]. \quad (30)$$

The TF approximation is valid in the limit of large N_c , where the energy contribution from the mean-field (Hartree) potential exceeds that of the kinetic energy. For this reason, Eq. (30) is not expected to be a good representation of the condensate density close to the transition temperature.

In the regime of small condensate numbers, therefore, it becomes more important to solve the equations for the condensate and excitations exactly in order to obtain the low-lying discrete states, as described in the preceding section. In this work, we use the exact GP and HFB equations, but the sum over discrete states is combined with an energy integral over high-lying states using LDA functions in the manner described by Reidl *et al.* [24]:

$$n_T(\mathbf{r}) = \sum_j n_j(\mathbf{r}) \Theta(\epsilon_c - \epsilon_j) + \int_{\epsilon_c}^{\infty} d\epsilon n_T(\epsilon, \mathbf{r}), \quad (31)$$

where $n_j(\mathbf{r})$ is the j th term of Eq. (9), ϵ_c is a low-energy cutoff, and, in the above notation, $n_T(\epsilon, \mathbf{r})$ has the form

$$n_T(\epsilon, \mathbf{r}) = \frac{m^{3/2}}{2^{3/2}\pi} \left[2\langle n(\mathbf{p}, \mathbf{r}) \rangle + 1 - \frac{\epsilon}{\mathcal{L}} \right] [\mathcal{L} - V_{\text{ext}} + \tilde{\mu} - 2gn]^{1/2}. \quad (32)$$

A similar equation applies to the anomalous average m_T . This latter hybrid procedure is referred to below as the discrete quasiparticle sum (DQS) approximation, an abbreviation for ‘‘discrete Hartree-Fock-Bogoliubov quasiparticle sum.’’ Either a Popov or $G2$ approximation may be made within the DQS, and these are referred to below as DQSP and DQSG, respectively.

A simpler LDA may be formulated by treating the local excitations within the Hartree-Fock approximation, which ignores the linear dispersion at low energies. The condensate density may again be obtained within the TF approximation using Eq. (30). The thermal density is given by $n_T(\mathbf{r}) = \int [d^3 p / (2\pi)^3] \langle n(\mathbf{p}, \mathbf{r}) \rangle$, where $\langle n(\mathbf{p}, \mathbf{r}) \rangle$ is defined in Eq. (28) but with $\epsilon(\mathbf{p}, \mathbf{r}) = \mathcal{L}(\mathbf{p}, \mathbf{r})$. Integration over the momenta readily yields

$$n_T(\mathbf{r}) = \frac{1}{\lambda_T^3} g_{3/2}(e^{-\beta[V_{\text{ext}}(\mathbf{r}) + 2gn(\mathbf{r}) - \mu]}), \quad (33)$$

where the thermal de Broglie wavelength is $\lambda_T = (2\pi\hbar^2/mkT)^{1/2}$ and $g_\alpha(z) = \sum_{j=1}^{\infty} z^j / j^\alpha$. As usual, the chemical potential μ is determined by the condition that the total atomic number $N = \int d\mathbf{r} [n_c(\mathbf{r}) + n_T(\mathbf{r})]$. With the TF expression (30) for the condensate, the argument of the $g_{3/2}$ function in Eq. (33) is always less than unity. If an ‘‘exact’’ solution for the condensate is used (i.e., obtained by solving the GP equation), the results are generally improved, but as noted below and in Ref. [17], there is then a range of temperatures $T \lesssim T_c$ for which the $g_{3/2}$ function given in Eq. (33) diverges, since its argument can become greater than unity.

An even simpler form of the LDA has been formulated [36,37] in which the effect of interactions on the excited states is completely ignored. Assuming a TF form for the ground state, this LDA consists of the parametrically coupled equations (in view of the other approximations here, in these equations we ignore the distinction between $\tilde{\mu}$ and μ):

$$n_c(\mathbf{r}) = \frac{\tilde{\mu} - V_{\text{ext}}(\mathbf{r})}{g} \Theta[\tilde{\mu} - V_{\text{ext}}(\mathbf{r})], \quad (34)$$

$$n_T(\mathbf{r}) = \frac{1}{\lambda_T^3} g_{3/2}(e^{-\beta[V_{\text{ext}}(\mathbf{r}) - \tilde{\mu}]}). \quad (35)$$

In this approximation, the interaction enters only via the chemical potential in the TF equation, which is a function of

a_{sc} and condensate number. For a spherical condensate, $\tilde{\mu}_{TF} = \frac{1}{2}(15N_c a_{sc}/a_0)^{2/5} \hbar \omega_0$, where $a_0 = \sqrt{\hbar/M\omega_0}$ is the bare oscillator length.

It is shown in Ref. [37] that a low-order expansion of Eq. (35) yields the following expression for N_0/N :

$$\frac{N_c}{N} = 1 - \left(\frac{T}{T_c^0}\right)^3 - \eta \frac{\zeta(2)}{\zeta(3)} \left(\frac{T}{T_c^0}\right)^2 \left(\frac{N_c}{N}\right)^{2/5}, \quad (36)$$

where $\zeta(n)$ is the Riemann zeta function, $\eta = \tilde{\mu}_{TF}/k_B T_c^0 \approx \frac{1}{2} \zeta(3)^{1/3} (15N_c^{1/6} a_{sc}/a_0)^{2/5}$, and the critical temperature for N ideal Bose atoms in a harmonic trap is given by [38,39]

$$k_B T_c^0 / \hbar \omega_0 = 0.9405N^{1/3} - 0.6842 + 0.50N^{-1/3}. \quad (37)$$

Equation (36) is solved iteratively for N_c/N .

E. Ideal Bose gas

Some of the plots given below contain results for ideal noninteracting Bose atoms ($a_{sc}=0$) in a harmonic trap. The results given for N_c were obtained from sums over the occupation numbers as given in Eq. (8), with $d_j = 2\ell_j + 1$, $E_j = \hbar \omega(\ell_j + 2n_j + 3/2)$. The chemical potential μ was adjusted to satisfy the condition $N = \sum_{j=0}^{\infty} \langle N_j \rangle$. An alternative expression can be obtained from the density distribution given by Chou *et al.* [40]:

$$N = \frac{z_1}{1-z_1} + \sum_{l=1}^{\infty} z_1^l \{ (1 - e^{-2l\beta}) [\tanh(\beta l/2)] \}^{-3/2} - 1, \quad (38)$$

where $z_1 = e^{\beta(\mu - 3/2)}$. This expression requires fewer terms than the aforementioned procedure, and gives identical results for temperatures up to about $0.9T_c$.

III. COMPUTATIONAL TECHNIQUES

With a spherically symmetric trapping potential, all observables may be decomposed into functions of radius r and spherical harmonics $\mathcal{Y}_l^m(\theta, \phi)$. The GP and Bogoliubov equations then become one-dimensional in r ; the ground state is assumed to have $(\ell, m) = (0, 0)$, while the excitations obtained using the Bogoliubov equations are $2\ell + 1$ degenerate. Both equations are solved using the discrete variable representation (DVR), a computationally efficient approach for the trapped interacting Bose gases that has been recently described in detail [25].

We have used two variants of the DVR approach: an equidistant mesh array derived from sine functions as discussed by Colbert and Miller [26], and a mesh based on Gaussian quadrature, using the zeros of associated Laguerre polynomials $L_{N_L}^\alpha(r)$, where N_L is the order of the quadrature and $\alpha = 2$ for a spherical condensate [27]. The latter DVR has the advantage of having a fine mesh for small r where the condensate density is nonzero, and a more coarse mesh at larger distances where the thermal distribution varies slowly. Although the condensate and excited orbitals are computed on the physical grid, the matrix elements of the operators are

represented by Laguerre polynomials up to the order defining the Gauss quadrature N_L , which in the present calculations range from 1000 to 2800; matrix elements of the kinetic energy are computed from expressions given in Ref. [27]. Increasing the value of N_L increases the accuracy of high-lying states, allowing for a larger cutoff energy ϵ_c at which the discrete sums are terminated, and a smaller number of atoms in the LDA integrals. Since high-order polynomials extend far beyond values of $R_{\max} \leq 50a_0$ relevant to trapped condensates, the number of spatial grid points required can be limited to just $N_g \sim 200$ for all values of N_L .

Implementation of the above mean-field theory requires a stable and efficient iteration procedure to solve the GP and Bogoliubov equations for a given total number of atoms N and temperature T . In our approach, the functions $n_c(r) = \Phi^2(r)$, $n_T(r)$, and $m_T(r)$ are calculated self-consistently using Eqs. (4) and (7)–(10), supplemented by the LDA expressions for states above the cutoff ϵ_c , for fixed N_c and T ; the chemical potential μ is determined by Eq. (18). Because this iteration procedure is especially delicate near T_c , yet is crucial for the results presented, we give a few more details.

We emphasize that the convergence criterion must consider the spatial distribution functions $n_c(\mathbf{r})$ and $n_T(\mathbf{r})$ rather than simply the aggregate values N_c and N_T . The iterative procedure can be decomposed into three separate levels of self-consistency, subject to the minimization of the ‘‘Error’’:

$$\text{Error} = \int d\mathbf{r} [|n_c^{\text{out}}(\mathbf{r}) - n_c^{\text{in}}(\mathbf{r})| + |n_T^{\text{out}}(\mathbf{r}) - n_T^{\text{in}}(\mathbf{r})|]. \quad (39)$$

The ‘‘in’’ and ‘‘out’’ functions are the input and output of the combined GP and HFB equations plus the high-energy LDA integral. Normally, the Error diminishes (though not necessarily monotonically) through level 1 iterations, in which the output functions are fed back into the GP, HFB, and high energy LDA equations. In this level, the condensate number N_c is held constant while the condensate density (normalized to unity) is allowed to vary. When the Error reaches some predetermined tolerance, level 2 iterations begin and N_c is adjusted to approach the condition that $N_c + N_T = N$. The first level 2 adjustment from the converged level 1 iterations is based on a simple proportionality between N and N_c . Subsequent level 2 adjustments are based on a linear relation between N_c and N , where the parameters are obtained from the last two level 2 iterations. After $N_c + N_T$ has converged to N to the desired tolerance, level 3 iterations proceed, in which iteration levels 1 and 2 are repeated with successively larger number of Laguerre functions N_L and mesh points N_g . These three levels of iteration typically achieve accuracies for the condensate number N_c of a few atoms. While this accuracy is beyond what is accessible to current experiments, it permits the comparison of different theoretical models.

The iteration procedure is illustrated in Fig. 1, which tracks a calculation for 2×10^5 atoms and scaled temperature $t = k_B T / \hbar \omega = 53$ [from Eq. (37), $t_c^0 \approx 54.3$], using the Laguerre DVR basis. After more than 50 iterations, N_c converged from the initial estimate of 109 to the final value of

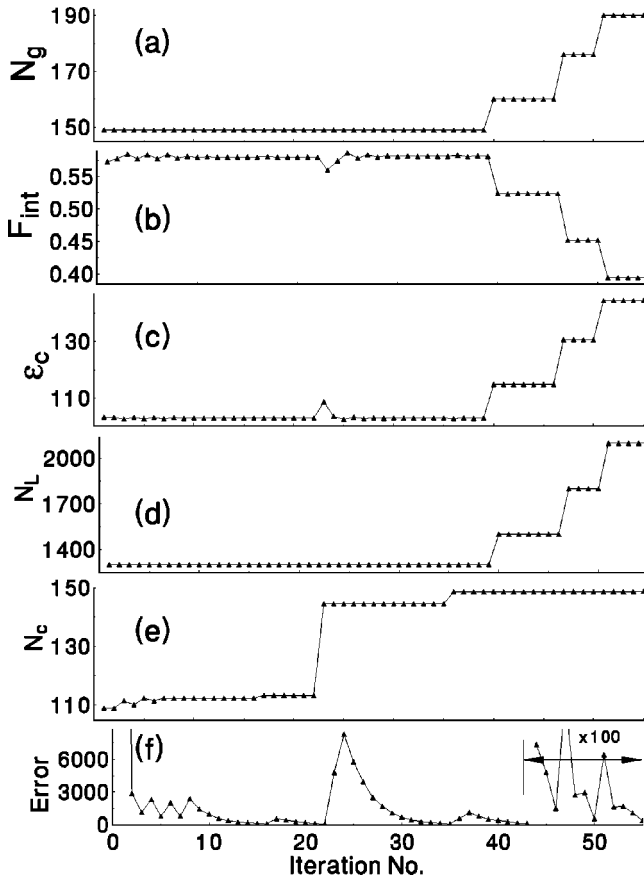


FIG. 1. Convergence of the self-consistency procedure, for $N = 2 \times 10^5$, $a_{sc}/a_0 = 0.0072$, $t_{sc} = 53$, and a Laguerre DVR mesh. (a) Number of points in the DVR mesh, N_g . (b) Fraction of atoms in the LDA integral, F_{int} . (c) Cutoff energy, ϵ_c , specifying the upper limit of the discrete quasiparticle sum. (d) Order of the Laguerre polynomial, N_L . (e) Condensate number N_c . (f) Error, defined by Eq. (39), showing convergence up to each change of N_c or N_g , and ultimately convergence to the condition that $N_c + N_T = N$.

149 atoms [Fig. 1(e)]. Each adjustment of N_c (level 2) or N_L (level 3) results in a jump in the error [Fig. 1(f)], which then converges again. In this calculation, N_L increased from 1300 to 2100 [Fig. 1(d)], corresponding to an increase of mesh points (up to $R_{max} = 42$) from 149 to 190 [Fig. 1(a)], an increase in ϵ_c from $102\hbar\omega_0$ to $144\hbar\omega_0$ [Fig. 1(c)], and a decrease in the fraction of the total number of atoms in the LDA integral from 57% to 40% [Fig. 1(b)].

The fraction of atoms in the LDA integral is negligible only for calculations at low temperatures with small N . Since T_c rises as $\sim 0.94N^{1/3}$, the required number of thermal states rises with N for calculations near T_c , and inevitably the LDA integration must include a larger fraction of atoms. For $N = 2 \times 10^4$, 2×10^5 , and 10^6 , at most 9%, 38%, and 74% of the atoms were in the integral at temperatures in the vicinity of T_c . Correspondingly, the mesh size N_g required to ensure convergence increased from 140 to 210 for N between 10^3 and 10^6 . The reason N_g does not increase more rapidly with N is that the LDA approximation improves with the total number of atoms.

It should be pointed out that for large values of N , the

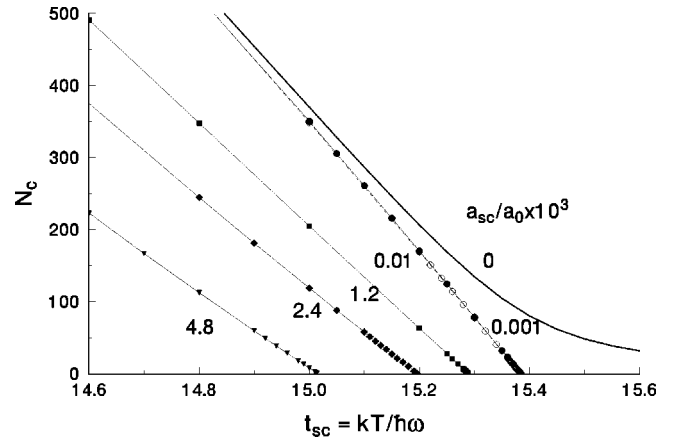


FIG. 2. If $\mu = \tilde{\mu}$, from the HFBP discrete quasiparticle sum (DQS) near T_c there is a discontinuity in the N_c vs T function with respect to a_{sc} . The figures show N_c vs T for $N = 5000$ atoms, for several values of a_{sc}/a_0 . Even in the limit of small a_{sc}/a_0 , N_c goes to zero abruptly with T for the self-consistent solution, while for the ideal Bose gas ($a_{sc} = 0$), $N_c(T)$ has a smooth tail.

iteration procedure could exhibit instabilities when the temperature approached T_c . For $N > 10^5$, we found that there often appeared to be (at least) two semistable regions when $N_c \leq 5000$, between which the calculation tended to fluctuate. In order to ensure the solution remained in the more stable state, small temperature increments $\Delta t = 0.2$ were used.

IV. THERMAL AVERAGES

A. Condensate fraction

In several of the plots to follow, results are presented for a series of values of a_{sc}/a_0 . For comparison with current experiments, we note that the scattering lengths a_{sc} for ^{87}Rb , ^{23}Na , and ^7Li are approximately given by $110a_B$, $52a_B$, and $-27.3a_B$, respectively, where $a_B \approx 5.292 \times 10^{-11}$ m is the Bohr radius. Thus, if one takes $\omega = (\omega_x \omega_y \omega_z)^{1/3}$, then for the recent MIT experiments [12] on ^{23}Na , $\nu = \omega/2\pi = 96.4$ Hz, the JILA experiments [9] give $\nu = 182.5$ Hz, and the Rice experiments [3] give $\nu = 144.6$ Hz, corresponding to $a_{sc}/a_0 = 0.00129$, 0.00729 , and -0.00046 , respectively.

Figure 2 illustrates the consequences of setting the eigenvalue of the GP equation $\tilde{\mu}$ equal to the chemical potential μ , as discussed in Sec. II A. With this assumption (here used in conjunction with the Popov approximation, $m_T = 0$), N_c goes to zero abruptly with T when the population in excited states reaches the total number of atoms $N = 5000$. By contrast, results for $a_{sc} = 0$, obtained as described in Sec. II E, have a smooth tail at high temperature. Thus, in the limit $a_{sc} \rightarrow 0$, the results near T_c exhibit a discontinuity with respect to the ideal gas results.

Figures 3 and 4 show results obtained from calculations in which the chemical potential is as given in Eq. (18). The smooth variation of the chemical potential, Fig. 3, through T_c is reflected in all relevant properties of the system, including the number of condensate atoms and excitation frequen-

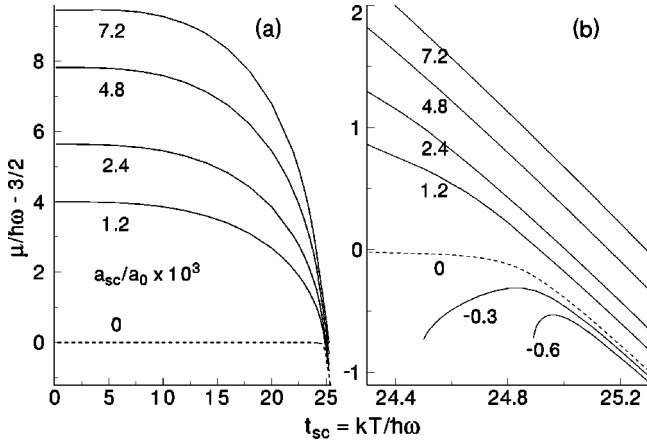


FIG. 3. The chemical potential in units of $\hbar\omega$ relative to the harmonic-oscillator zero-point energy, $\mu/\hbar\omega - 3/2$, vs T for various values of a_{sc}/a_0 . (a) shows the full range of temperatures up to T_c , while (b) shows a limited range near T_c .

cies. When $a_{sc} > 0$, the chemical potential evolves continuously from positive to negative values, relative to the harmonic-oscillator zero-point energy $\frac{3}{2}\hbar\omega$, as the temperature increases. Since μ increases with the interaction strength, the value at which the chemical potential passes

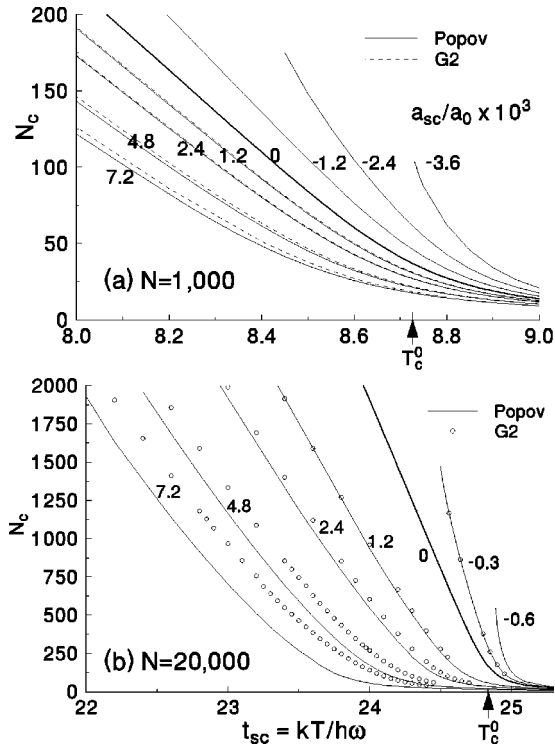


FIG. 4. When μ differs from $\tilde{\mu}$ according to Eq. (18), the N_c vs T function from the discrete quasiparticle sum behaves smoothly with respect to a_{sc} . Shown are the results for (a) $N=1000$ and (b) $N=20000$ atoms. The critical temperature for $a_{sc}=0$, defined as the maximum of d^2N_c/dT^2 , is indicated with an arrow. For $a_{sc} < 0$ the maximum value of N_c is limited due to the instability of the condensate. In (b), open circles denote results obtained with the G2 approach.

through zero increases with a_{sc} even though T_c decreases. In addition, Fig. 3 shows that for $a_{sc} < 0$, $\mu < 3\hbar\omega/2$ everywhere, with maximum values at temperatures $T \sim T_c$.

Figure 4 shows the number of condensate atoms as a function of temperature for $N=1000$ and 20000 for a range of interaction strengths a_{sc}/a_0 , calculated within the DQS formalism. The condensate population near T_c is evidently a continuous function of both the scattering length and temperature.

The plots shown in Fig. 4, especially for 20000 atoms, show that the $G2$ renormalization procedure results in a significantly higher value of N_c , relative to that obtained within the Popov approximation, for the larger values of a_{sc} . Furthermore, the difference between the $G2$ and Popov results becomes more pronounced as a_{sc} increases. This behavior is consistent with expectation because $G2$ produces a weakening of the atom-atom interaction. The use of the occupation factors (16) rather than Eq. (8) also increases the value of N_c by a few atoms at high temperatures, but the effect is much smaller than what results from the use of $G2$ theory.

For $a_{sc} < 0$, the N_c values reach a maximum when the calculation becomes numerically unstable [41–44], reflecting the physical instability of the cloud towards spatial collapse. The maximum N_c values depend on a_{sc} , as shown by the termination of the curves for these cases. For $T=0$, the maximum value is given by $N_c^{\max} = 0.573a_0/a_{sc}$ [41]. This critical number is known to decrease when $T > 0$ due to the presence of thermal atoms [42,43]. In these plots, the maximum N_c is 80% to 57% of the value calculated for $T=0$, confirming that the thermal cloud significantly decreases the stability of the condensate for $a_{sc} < 0$.

B. Comparison with LDA and QMC

It is interesting to explore how our finite-temperature results compare with those obtained by other methods. Local-density approximations are much simpler to implement numerically than the full self-consistent HFB equations and their variants. The opposite is true of Monte Carlo calculations, but these do not invoke the mean-field approximation, and therefore yield results for equilibrium configurations that are essentially exact.

Figure 5 for $N=2 \times 10^4$ compares N_c values from the Popov and $G2$ quasiparticle sums (DQSP and DQSG) with several LDA methods. Our Hartree-Fock LDA (HFLDA) solves the GP equation for the condensate $n_c(r)$, iterated to self-consistency using Eq. (33) for the thermal distribution $n_T(r)$. We found it most efficient to start at low temperature, in order to obtain good initial estimates of $n_T(r)$ at successively higher values of T . No solution could be found for $N_c/N < 0.035$ due to the failure of the HFLDA, as discussed above and in Ref. [17].

The “semi-ideal” LDA (SILDA) [37] omits the $n_T(r)$ term in the TF expressions for the condensate (30) and for the total density $n_T(r)$ in Eq. (33). This results in the simple expressions (35) which are related solely through the chemical potential. Iterative solution of these equations yields results that are close to the other functions plotted in Fig. 5. The actual $n_T(r)$ distribution calculated with this approach

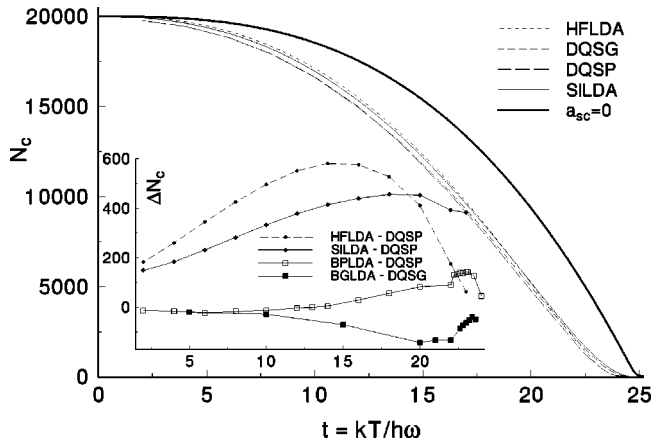


FIG. 5. Comparison of values for N_c/N from quasiparticle sums with the Popov and $G2$ approximations, as compared with HFLDA and SILDA for $N=20000$ atoms and $a_{sc}/a_0=0.0072$. BLDA results are too close to distinguish on this scale. On an expanded scale, the inset gives differences between indicated LDA and DQS methods.

exhibits a sharp peak at the edge of the condensate due to the discontinuity at the Thomas-Fermi condensate radius.

The inset of Fig. 5 shows that the Hartree-Fock Bogoliubov LDA methods, BPLDA and BGLDA, agree most closely with the hybrid method, DQSP and DQSG, respectively. The two BLDA methods employ a TF condensate, and thus the $n_T(\mathbf{r})$ functions exhibit a small spike at the edge of the condensate, which has a cusp. As with the HFLDA, the calculations required iteration to self-consistency, which was facilitated when initial values were obtained by extrapolation from results from lower-temperature values.

It is remarkable that the values for N_c from BLDA calculations agreed with the corresponding DQS results to better than 0.4% of N in every case for which results were obtained. Even for HFLDA and SILDA, the differences with DQS results are less than the fractional error in current experiments. Thus these comparisons show that relatively simple LDA expressions are useful for obtaining the condensate fraction as a function of temperature. It is only in the region near T_c and above, where the condensate number becomes small, that our LDA methods failed.

The quantum Monte Carlo (QMC) approach uses the exact Hamiltonian with a hard-sphere atom-atom interaction. Based on extensive numerical experience with ^4He [22], QMC should be most useful for the calculation of equilibrium quantities, such as the condensate fraction. Holzmann *et al.* [17] have provided benchmark QMC calculations for the case of 10^4 Bose atoms confined in a spherical trap, with $a_{sc}/a_0=0.0043$. Table I shows comparisons between our results and those of QMC [17,45] for the condensate number as a function of temperature. The DQSP, DQSG, and QMC values differ by up to 1.2% of the total atom number N . It is notable that at higher temperatures, N_c falls off less quickly using HFBP and $G2$ than QMC. This may be due in part to the fact that the relationship between N_c and μ in Eq. (18) is not entirely correct at higher temperatures, as discussed in Sec. II B, and may resemble ideal-gas statistics too closely.

TABLE I. Comparison of condensate numbers, n_0 , obtained from quantum Monte Carlo calculations and from this work, with and without atom-atom interactions, and results obtained here from discrete Bogoliubov quasiparticle sums and discrete Hartree-Fock sums. The error limits for QMC are of course purely positive for $n_0=0$.

$T/\hbar\omega$	QMC N_c	DQSG N_c	DQSP N_c	HFLDA ^a N_c	HFLDA ^b N_c
16.667	2265(10)	2213	2159	2216	2222
16.949	1971(10)	1936	1883	1945	1935
17.242	1656(15)	1654	1599	1630	1638
17.544	1374(10)	1367	1309	1323	1333
17.857	1057(10)	1072	1016	1008	1022
18.182	741(10)	782	726	686	
18.519	440(10)	501	448		
18.868	180(10)	247	205		
19.231	21(11)	140	57		
19.608	0(20)	71	21		
19.802	0(20)		15		
20.0	0(10)		12		
20.202	0(14)		9		

^aHolzmann *et al.* [17,45].

^bThis work, using Eq. (35).

Presumably the many-body effects that necessitate the renormalization of the atom-atom interaction are already included in the QMC procedure, in which case results with $G2$ should be closer than Popov to the QMC. Indeed, for $t=k_B T/\hbar\omega < 17.3$, the Popov results lie below QMC, while the $G2$ numbers are higher and closer to QMC. Above a scaled temperature $t=17.8$, however, the $G2$ results rise above QMC values.

C. Critical temperature versus a_{sc}

Figures 4 and 5 show that large values of a_{sc} have the effect of flattening the curve of condensate number as a function of temperature, as is already apparent in the plots of Giorgini *et al.* [36]. If these curves are fit to a function $N_c/N=1-(T/T_c)^\alpha$, one obtains values for α as low as 1.4, compared with the ideal-gas value of 3. Another parameter to characterize the effect of atom-atom interactions is the shift of the critical temperature from the ideal Bose gas case. For the homogeneous Bose gas, where it is uniquely defined as the point at which N_c goes to zero, this shift has been the subject of intense discussion recently [46]. For atoms in a harmonic potential, as is especially clear in Fig. 4, this point is not sharp (indeed, the number of condensate atoms is finite at all temperatures in a mesoscopic system). Definitions of T_c that have been proposed include the point at which the density at the origin reaches the critical density for a homogeneous gas [47], the maximum of the specific heat, and the maximum of the temperature derivative of the specific heat [39]. Since such energy-weighted properties pose additional problems for numerical calculations of thermal averages, T_c is determined here as the maximum of the function d^2N_c/dT^2 . The inflection point of the N_c versus T function, or zero of d^2N_c/dT^2 , deviated from Eq. (37) by a significantly larger amount.

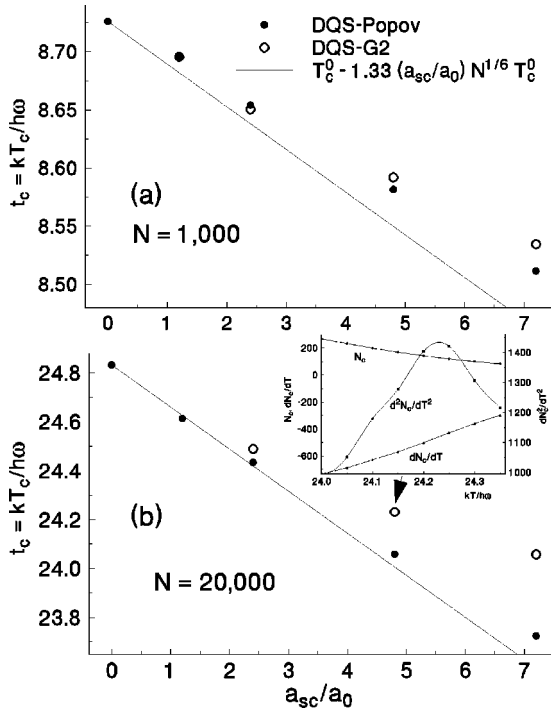


FIG. 6. Values for the critical temperature, T_c , defined as the maximum of $d^2 N_c / dT^2$. Results are shown for (a) $N = 1000$ and (b) $N = 20\,000$ atoms, for the DQSP and DQSG approaches. The solid line represents the semiclassical prediction $T_c = T_c^0 - \Delta T_c$, where T_c^0 is the transition temperature in the noninteracting limit. The inset in (b) shows the $N_c(T)$, $N_c(T)/dT$, and $d^2 N_c / dT^2$ functions from which T_c is determined for the cases $a_{sc}/a_0 = 0.0048$, the last with a spline fit.

Figure 6 shows T_c values extracted from the data used in Fig. 4. For comparison, the ideal-gas data are analyzed in a similar manner, yielding values of T_c that are close to, but not identical with, those obtained using Eq. (37). Figures 6(a) and 6(b) correspond to 1000 and 20 000 atoms, respectively. The inset in Fig. 6(b) shows how the transition tem-

perature is determined from the data in a typical case, by making use of the three functions $N_c(T)$, $dN_c(T)/dT$, and $d^2 N_c / dT^2$. Since both the condensate number and its temperature derivative are nearly straight lines, accurate calculation of the second derivative requires accurate numeric values of these functions.

A semiclassical analysis by Giorgini *et al.* [48] indicates that the transition temperature should decrease linearly from the ideal-gas value with increasing particle interactions. The results of the DQS-Popov calculations confirm this general scaling; furthermore, as the number of atoms increases, the observed shift in the critical temperature δT_c matches the semiclassical expression more closely at larger a_{sc}/a_0 . In contrast, with the DQS-G2 approach δT_c shows significant deviations from linear scaling for small N , and these become more pronounced as the number of atoms increases. For $N = 2 \times 10^4$, the shifts are significantly less than the semiclassical values for the larger values of a_{sc}/a_0 considered.

D. Renormalization of the atom-atom interaction

As indicated in Fig. 4, the G2 renormalization yields values for N_c/N that reflect the weakening of the atom-atom repulsion; at any given temperature, the number of atoms in the condensate increases relative to the value obtained using the Popov approximation. Perhaps more interesting is the spatial variation of the effective interaction in the harmonic trap. The renormalization is governed by the local value of m_T relative to n_c . In general, $|m_T|$ increases with the number of noncondensed atoms n_T since more terms enter the sum (10); however, m_T vanishes when $n_c = 0$, since the “quasi-hole” amplitude $v_i = 0$. In general, therefore, one might expect the local renormalized interaction to reach a minimum at some temperature. For a uniform Bose gas, this minimum occurs at exactly the transition temperature, and corresponds to a vanishing of the effective scattering length [20,21].

In Fig. 7 we compare the condensate and thermal densities with the spatial variations of the anomalous average and

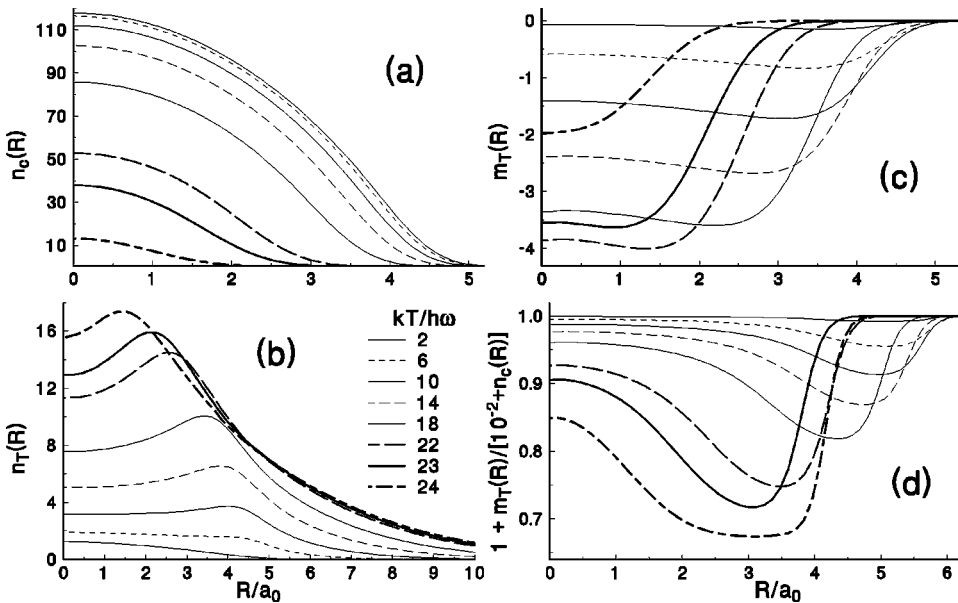


FIG. 7. The functions $n_c(r)$, $n_T(r)$, $m_T(r)$, and $g(r)/g$ are shown for $N = 20\,000$ atoms, $a_{sc}/a_0 = 0.0072$ over a wide range of temperatures. $|m_T(r)|$ is largest at the edge of the condensate and increases with T up to T_c .

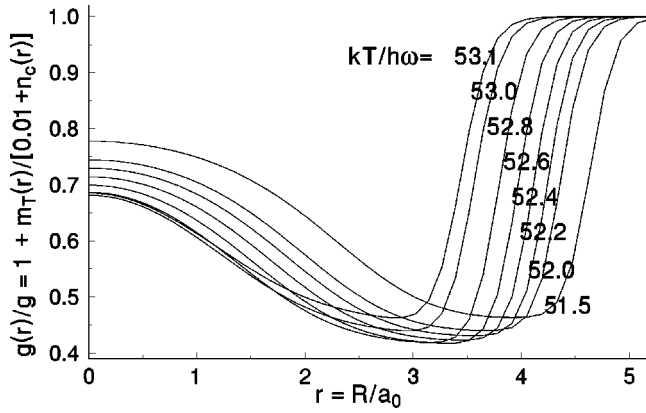


FIG. 8. Variation of the renormalization factor, $g(r)/g$, with temperature near T_c for $N=200\,000$ and $a_{sc}/a_0=0.0072$. The range of the minimum decreases as the condensate shrinks with T , while the minimum value continues to decrease up to a point, and then increases.

the effective particle interactions for the case of $N=20\,000$ and $a_{sc}/a_0=0.0072$ for various temperatures. (As noted above, this would correspond to a relatively tight trap for ^{23}Na .) For these plots, $\delta=0.01$ in Eq. (25). There is a slight dependence of the results on δ , since much smaller values $\delta\sim 10^{-4}$ lead to a small bump in the $m_T(r)$ function at the very edge of the condensate. The dependence on this arbitrary parameter indicates an ambiguity in the theory; however, the integrated numbers are not significantly altered by the choice of δ , since the errors are incurred in regions of very small condensate density.

The manner in which $g(r)/g$ attains a minimum in r is shown in Fig. 8 for the particular case of $N=2\times 10^5$. The global minimum occurs at a temperature close to T_c , defined above. Following this procedure, we consider the $g_{\min}(r)/g$ functions for various values of N for $a_{sc}/a_0=0.0072$, which are displayed in Fig. 9. Though we have increased N without changing a_{sc}/a_0 , the approach to the thermodynamic limit is

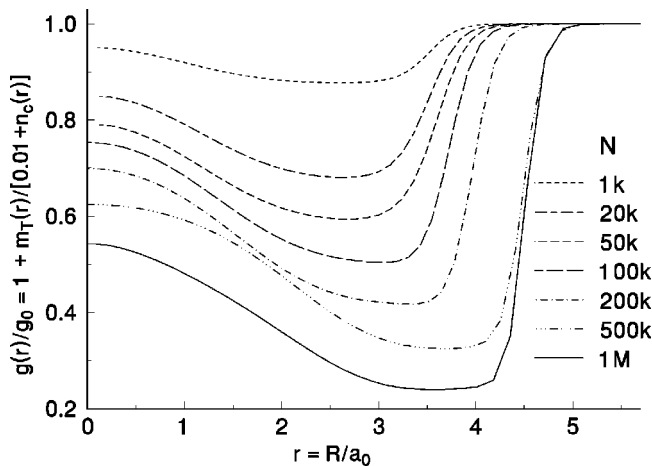


FIG. 9. The curves shown are the “minimum” functions, $g_{\min}(r)/g$, as a function of temperature (such as shown in the previous figure) for each N value given. These curves are for $a_{sc}/a_0=0.0072$.

beginning to emerge. The minimum for each N is found to always occur very close to the calculated transition temperature, and its value decreases approximately with $\log_{10}(N)$ over the range of N considered. For $N=10^6$, we obtain $g_{\min}(r)/g\approx 0.2$. It should be noted that although the fraction of total atoms in the LDA integral increased to approximately $\frac{3}{4}$ for $N=10^6$ near T_c , the high-energy LDA contribution to m_T was in every case less than 2%, and typically an order of magnitude less than this value.

It should be emphasized that the $G2$ renormalization employed in the present calculations is derived for a uniform Bose gas, and should best represent large condensate densities or low temperatures where the LDA is most applicable. While the LDA is bound to fail for $T\rightarrow T_c$, the regime where it loses validity will become smaller with increasing N , and should approach the critical region where perturbation theory itself breaks down. It would be preferable to define the renormalization of the particle interactions in terms of the full many-body T matrix in a trap, and we hope to pursue this issue in future work. The $G2$ approach as formulated above, however, should properly describe the effects of two-body correlations for large trapped condensates at low to intermediate temperatures. Thus, the strong reduction in the effective interaction strength over much of the condensate, indicated by the $G2$ theory, could have significant experimental consequences. The predictions for the excitation frequencies are discussed further below.

E. Excitation frequencies

The quasiparticle eigenvalues correspond to excitation frequencies, but it remains unclear what relationship exists between these values and experimentally observed resonances of the trapped gas at finite temperatures when the potential of a harmonic trap is perturbed periodically. In all mean-field calculations such as those presented here, the linear-response equations assume that the thermal density is fixed, while in experiments it would also be perturbed. For this reason, the dipole excitation frequency obtained within mean-field theories will generally not satisfy the generalized Kohn theorem [49], which states that there is a mode in which the entire ensemble oscillates at the bare trap frequency. Calculations explicitly including the dynamics of both n_c and n_T [13,14] are found to be consistent with the Kohn theorem.

Figure 10 shows small but significant deviations in the Kohn mode from unity for $N=2\times 10^4$ and 2×10^5 , both within the DQS-Popov and DQS- $G2$ approaches. That the $G2$ frequency should be lower than the Popov value cannot be simply understood in terms of an overall decrease in the interatomic repulsion, since this would predict a mode closer to unity. Rather, the spatial variation of the effective interaction leads to a flattening of the effective potential, comprised of the trap plus the Hartree potential; the looser effective confinement softens all the modes. We are not aware of other computational results in which the Popov value starts from below unity and rises above, before falling near T_c . This behavior may be a consequence of a more rigorous treatment of the chemical potential, Eq. (18). Alternatively, since the

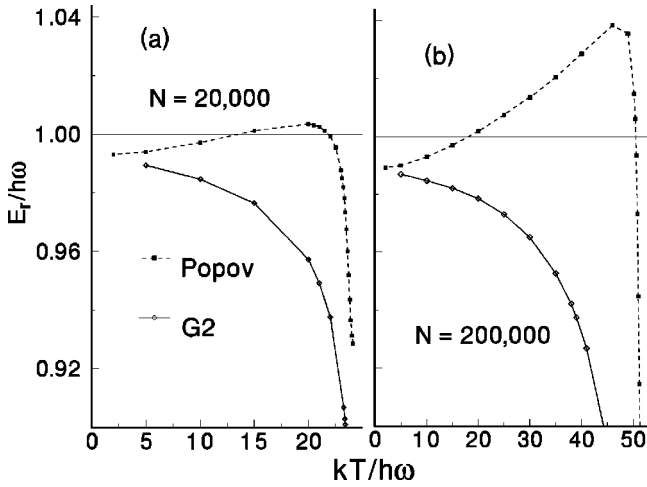


FIG. 10. Excitation frequencies of the lowest $\ell=1$ mode in comparison with the Kohn theorem value of unity. Results from the Popov (dashed lines) and $G2$ (solid lines) approximations are shown for (a) $N=2 \times 10^4$ and (b) $N=2 \times 10^5$. All results are for $a_{sc}/a_0=0.0072$.

differences increase with N (specifically, the noncondensate density), they may not have been observable with the smaller N values studied previously.

The temperature dependence of the low-lying excitation frequencies obtained with the DQSP and DQSG approaches is shown in Fig. 11 for $N=2 \times 10^4$ and 2×10^5 . The softening of all the excitation frequencies in the $G2$ approximation was found previously by the proponents of this theory [11] (for a “pancake” geometry) as well as by others using a similar perturbative approach to the interacting Bose gas [50]. However, for a spherically symmetric trap, the results of Ref. [11] for 2000 Rb atoms showed only a negligible difference between Popov and $G2$ excitation frequencies. The present results show that for a spherically symmetric trap and larger atom numbers, there can be differences between the Popov and $G2$ values that would be experimentally detectable. These results also lead to the question of

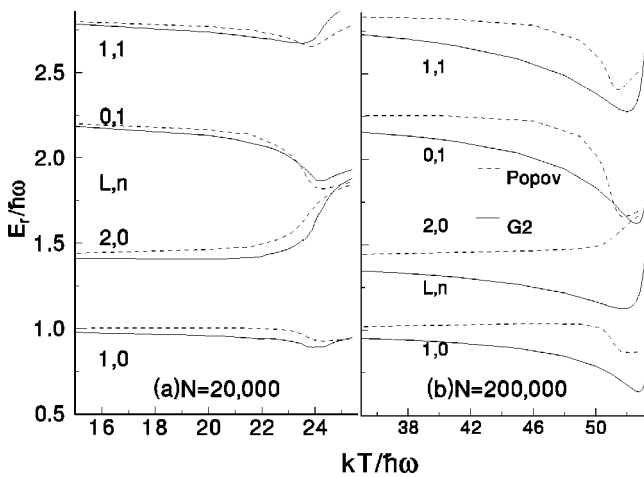


FIG. 11. Excitation frequencies for the lowest $\ell=0, 1$, and 2 modes for (a) $N=2 \times 10^4$ and (b) $N=2 \times 10^5$ within the Popov (dashed lines) and $G2$ (solid lines) models, where $a_{sc}/a_0=0.0072$.

whether for larger atom numbers a renormalized atom-atom interaction would effect frequencies calculated by the methods of Refs. [13,14], which did *not* assume a static condensate. It should also be mentioned that experimentally observed excitation frequencies with larger numbers of sodium atoms in a “cigar” geometry [12] also exhibited a softening of both the quadrupole and *dipole* excitation frequencies as the temperature approaches T_c .

V. DISCUSSION AND CONCLUSIONS

In this work, we have extended finite-temperature mean-field calculations for Bose-Einstein condensates confined in harmonic traps [8,11]. A careful derivation of the mean-field equations provides improved definitions of the thermodynamic chemical potential and quasiparticle occupation factors, yielding observables that are continuous functions of the particle interactions. The numerical techniques employed in the calculations have allowed for the investigation of systems with the large numbers of atoms relevant to ongoing experiments. In the process, we have been able to make several crucial comparisons between the results of evaluating discrete summations over quasiparticle states (which are numerically time-consuming) and various local-density approximations. Furthermore, we have explored the implications of a recently proposed gapless theory which takes into account pairing correlations.

The results presented above indicate a significant inadequacy of conventional static mean-field theory for computations of excitation frequencies of trapped Bose condensates at finite temperatures. For a large number of atoms and interaction strength, we find appreciable deviations of the dipole frequency obtained with either the Popov or $G2$ approximations from expectations of the generalized Kohn theorem. In our computations, the condensate is static in the presence of thermal excitations. The excited dipole mode corresponds approximately to out-of-phase motion of the thermal cloud relative to the condensate, as observed experimentally [12] when the dipole mode of the thermal cloud is excited separately. Detailed modeling of such excitation modes has been performed only by restrictive parametrization of the condensate and thermal cloud in the collisionless [14] or hydrodynamic [13] regimes. Both of these approaches address the two-fluid nature of these systems, and produce dipole modes that satisfy the Kohn theorem exactly. We will argue that equilibrium thermal excitations are computed accurately by the mean-field DQS methods presented here. However, any experimental probe of these excitations involves perturbative processes that require other theoretical methods.

In principle, mean-field theories that include fluctuations in the population of excited states [16,51] ought to be equivalent to the two-fluid dynamics in the collisionless regime. A full second-order perturbation theory of the interacting Bose gas should yield the coupled modes of the condensate and thermal clouds as well as damping rates. Indeed, employing the approximate many-body T matrix in the calculations (the $G2$ approximation described above) yields excitations that have a temperature dependence qualitatively

similar to that of out-of-phase modes. We hope to explore these issues in future work.

ACKNOWLEDGMENTS

This work was supported by the National Science Foundation (T.B. and B.I.S.), the Office of Naval Research (T.B. and D.L.F.), and by a grant from the NCF-Cray Foundation

of the Netherlands (T.B.). The authors are grateful for valuable conversations with H. Beijerinck, K. Burnett, C. W. Clark, K. K. Das, M. Doery, M. Edwards, M. Gajda, A. Griffin, D. A. W. Hutchinson, H. Metcalf, H. Stoof, E. Vredenbregt, and E. Zaremba. The authors particularly appreciate S. A. Morgan for his valuable comments and for sending us a preliminary draft of his D.Phil. thesis.

-
- [1] M.H. Anderson, J.R. Ensher, M.R. Matthews, C.E. Wieman, and E.A. Cornell, *Science* **269**, 198 (1995).
- [2] K.B. Davis, M.O. Mewes, M.R. Andrews, N.J. van Druten, D.S. Durfee, D.M. Kurn, and W. Ketterle, *Phys. Rev. Lett.* **75**, 3969 (1995).
- [3] C.C. Bradley, C.A. Sackett, J.J. Tollett, and R.G. Hulet, *Phys. Rev. Lett.* **75**, 1687 (1995); C.C. Bradley, C.A. Sackett, and R.G. Hulet, *ibid.* **78**, 985 (1997).
- [4] K. Huang, *Statistical Mechanics* (Wiley, New York, 1963).
- [5] L.D. Landau and E.M. Lifshitz, *Statistical Physics* (Addison-Wesley, Reading, MA, 1958).
- [6] F. Dalfovo, S. Giorgini, L. Pitaevskii, and S. Stringari, *Rev. Mod. Phys.* **71**, 463 (1999).
- [7] A.S. Parkins and D.F. Walls, *Phys. Rep.* **303**, 1 (1998).
- [8] D.A.W. Hutchinson, E. Zaremba, and A. Griffin, *Phys. Rev. Lett.* **78**, 1842 (1997).
- [9] D.S. Jin, M.R. Matthews, J.R. Ensher, C.E. Wieman, and E.A. Cornell, *Phys. Rev. Lett.* **78**, 764 (1997).
- [10] R.J. Dodd, M. Edwards, C.W. Clark, and K. Burnett, *Phys. Rev. A* **57**, R32 (1998).
- [11] D. Hutchinson, R. Dodd, and K. Burnett, *Phys. Rev. Lett.* **81**, 2198 (1998).
- [12] D.M. Stamper-Kurn, H.-J. Miesner, S. Inouye, M.R. Andrews, and W. Ketterle, *Phys. Rev. Lett.* **81**, 500 (1998).
- [13] E. Zaremba, A. Griffin, and T. Nikuni, *Phys. Rev. A* **57**, 4695 (1998); T. Nikuni, E. Zaremba, and A. Griffin, *Phys. Rev. Lett.* **83**, 19 (1999); E. Zaremba, T. Nikuni, and A. Griffin, *J. Low Temp. Phys.* **116**, 277 (1999); M. Milena Imamović-Tomasović, and A. Griffin, *Phys. Rev. A* **60**, 494 (1999).
- [14] M.J. Bijlsma and H.T.C. Stoof, *Phys. Rev. A* **60**, 3973 (1999).
- [15] A. Griffin, *Phys. Rev. B* **53**, 9341 (1996).
- [16] N.P. Proukakis, S.A. Morgan, S. Choi, and K. Burnett, *Phys. Rev. A* **58**, 2435 (1998).
- [17] M. Holzmann, W. Krauth, and M. Naraschewski, *Phys. Rev. A* **59**, 2956 (1999).
- [18] M. Bijlsma and H.T.C. Stoof, *Phys. Rev. A* **55**, 498 (1997).
- [19] S. Morgan, D.Phil. thesis, Oxford University, 1999.
- [20] M. Bijlsma and H.T.C. Stoof, *Phys. Rev. A* **54**, 5085 (1996).
- [21] H. Shi and A. Griffin, *Phys. Rep.* **304**, 1 (1998).
- [22] D.M. Ceperley, *Rev. Mod. Phys.* **67**, 279 (1995).
- [23] W. Krauth, *Phys. Rev. Lett.* **77**, 3695 (1996).
- [24] J. Reidl, A. Csordás, R. Graham, and P. Szépfalussy, *Phys. Rev. A* **59**, 3816 (1999).
- [25] B.I. Schneider and D.L. Feder, *Phys. Rev. A* **59**, 2232 (1999).
- [26] D. Colbert and W. Miller, *J. Chem. Phys.* **96**, 1982 (1992).
- [27] D. Baye and P.-H. Heenan, *J. Phys. A* **19**, 2041 (1986).
- [28] A.L. Fetter, *Ann. Phys. (N.Y.)* **70**, 67 (1972).
- [29] A.L. Fetter, *Phys. Rev. A* **53**, 4245 (1996).
- [30] A.L. Fetter, e-print cond-mat/9811366 (1998).
- [31] Z. Idziaszek, M. Gajda, P. Navez, M. Wilkens, and K. Rzążewski, *Phys. Rev. Lett.* **82**, 4376 (1999).
- [32] S. Giorgini, L.P. Pitaevskii, and S. Stringari, *Phys. Rev. Lett.* **80**, 5040 (1998).
- [33] Y.-S. Wu, *Phys. Rev. Lett.* **73**, 922 (1994).
- [34] R.K. Bhaduri, S.M. Reimann, A.G. Choudhury, and M.K. Srivastava, e-print cond-mat/9908210.
- [35] F.D.M. Haldane, *Phys. Rev. Lett.* **67**, 937 (1991).
- [36] S. Giorgini, L. Pitaevskii, and S. Stringari, *J. Low Temp. Phys.* **109**, 309 (1997).
- [37] M. Naraschewski and D. Stamper-Kurn, *Phys. Rev. A* **58**, 2423 (1998).
- [38] S. Grossmann and M. Holthaus, *Z. Naturforsch. Teil A* **50a**, 921 (1995).
- [39] N. Balazs and T. Bergeman, *Phys. Rev. A* **58**, 2359 (1998).
- [40] T.T. Chou, C.N. Yang, and L.H. Yu, *Phys. Rev. A* **53**, 4257 (1996).
- [41] P. Ruprecht, M.J. Holland, K. Burnett, and M. Edwards, *Phys. Rev. A* **51**, 4704 (1995).
- [42] M. Houbiers and H.T.C. Stoof, *Phys. Rev. A* **54**, 5055 (1996).
- [43] M.J. Davis, D.A.W. Hutchinson, and E. Zaremba, *J. Phys. B* **32**, 3993 (1999).
- [44] T. Bergeman, *Phys. Rev. A* **55**, 3658 (1997); **56**, 3310(E) (1997).
- [45] We thank M. Holzmann for sending us the numerical values used for Fig. 3 of Ref. [8].
- [46] G. Baym, J.-P. Blaizot, M. Holzmann, F. Laloë, and D. Vautherin, *Phys. Rev. Lett.* **83**, 1703 (1999); M. Holzmann and W. Krauth, *Phys. Rev. Lett.* **83**, 2687 (1999); K. Huang, *ibid.* **83**, 3770 (1999); G. Baym, J.-P. Blaizot, and J. Zinn-Justin, *Europhys. Lett.* **49**, 150 (2000).
- [47] M. Houbiers, H.T.C. Stoof, and E.A. Cornell, *Phys. Rev. A* **56**, 2041 (1997).
- [48] S. Giorgini, L.P. Pitaevskii, and S. Stringari, *Phys. Rev. A* **54**, 4633 (1996).
- [49] J. Dobson, *Phys. Rev. Lett.* **73**, 2244 (1994).
- [50] J. Reidl, A. Csordás, R. Graham, and P. Szépfalussy, *Phys. Rev. A* **61**, 043606 (2000).
- [51] S. Giorgini, *Phys. Rev. A* **57**, 2949 (1998).